

ETP sludge as filler and the role of AOD slag & GBFS in fly ash–slag–sludge blended geopolymers

Abstract

The Effluent Treatment Plant Sludge (ETPS) obtained from wire drawing industry has been used as a filler material in fly ash–slag based geopolymers. Argon Oxygen Decarburization (AOD) slag from steel making plant and Granulated Blast Furnace Slag (GBFS) from iron industry have been used for making two different blends. The work investigates the potential of ETPS as filler and the Role of AOD slag & GBFS in fly ash–slag–sludge (FA+AOD+ETPS & FA+GBFS+ETPS) blended geopolymers. The characterization of raw materials was done using Inductive Coupled Plasma (ICP) technique, Sieve analysis, and X-Ray Diffractometry (XRD). The alkaline activator used for the activation of the ternary blend was the combination of NaOH and Na–silicate. The concentration of NaOH and the ratio of Na–silicate to NaOH were fixed to 6 M and 0.33 respectively. The curing temperature and curing period used for geopolymer synthesis were 50 °C and 24 h. GBFS based samples showed higher strength than AOD based samples. The compressive strength was in the range of 3.8 to 17.5 MPa. GBFS based samples showed better resistance towards acid attack than AOD based samples. The early geopolymerization were analyzed at 27 °C using Isothermal Conduction Calorimetry (ICC). The results showed that GBFS based samples had an intense peak at a lower time than AOD based samples. The characterization of hardened geopolymers samples by XRD and SEM–EDAX revealed that the major reaction products are N–A–S–H, C–A–S–H or (N, C)–A–S–H and C–S–H gel.

Keywords: ETP sludge, fly ash–slag–sludge blended geopolymers, strength, durability, geopolymerization, microstructure

Introduction

Geopolymer is a revolutionary building material of modern era. The synthesis of geopolymer is done by using materials rich in amorphous silica (SiO_2) & alumina (Al_2O_3) with an alkaline activator.^{1–3} Different types of Industrial by-products are increasingly used as source materials for geopolymers.^{4–7} Few of them are Fly Ash (FA) from the coal-based thermal power plant, Granulated Blast Furnace Slag (GBFS) from iron industry, Argon Oxygen Decarburization (AOD) Slag from steel making plant, etc. Utilization of fly ash and GBFS in making geopolymer has been well established.^{7,8} Few authors also report the utilization of AOD slag in geopolymer synthesis.⁹ AOD slag contains a high amount of CaO, which limits the use of AOD slag in geopolymer synthesis. Salman et al.,⁹ reports that the maximum strength of AOD slag based geopolymers was 21 MPa and 30 MPa when activated with Na–silicate & 5M NaOH and K–silicate & 5M KOH respectively and steam cured at 80°C for 24 h. But the potential of Effluent Treatment Plant Sludge (ETPS), which is generated from various industries such as textile industry, wire drawing industry, etc., has not been studied in making geopolymer. ETPS is openly dumped, which leads to the soil, surface water, and groundwater contamination.¹⁰ ETPS contains a very high amount of iron and lacks the presence of silica, alumina or lime. Hence, it cannot be used as source material in making geopolymers. Few researchers have reported the potential of industrial ETPS in making cement concrete.^{11,12} The current paper presents the study on the potential of ETPS as a filler material in making fly ash–slag based geopolymers and also presents the comparative study of the role of AOD slag and GBFS in fly ash–slag–sludge blended geopolymers. The characterization of starting materials was done using Inductive Coupled Plasma (ICP) technique, Sieve analysis, and X–Ray Diffractometry (XRD). The geopolymerization reaction was recorded on Isothermal Conduction Calorimeter (ICC). The mineralogical characteristic of hardened geopolymers samples

was studied using powder X–Ray Diffractometry (XRD) and the morphology was studied using Scanning Electron Microscopy with Energy Dispersive X–ray spectroscopy (SEM–EDAX).

Materials and methods

Materials

Fly ash was collected from Tata Power Limited, Jharkhand, India. Granulated Blast Furnace Slag (GBFS) was collected from Tata Steel, Jamshedpur, India. Argon Oxygen Decarburization (AOD) Slag was collected from Jindal Steel & Power Limited, Jajpur, Odisha, India. Effluent Treatment Plant Sludge (ETPS) was collected from Usha Martin Ranchi Unit, Jharkhand, India. Fly ash was used as feedstock to form an alumino–silicate gel during geopolymerization, whereas ETPS was used as filler material in blended geopolymers. GBFS and AOD slag were added for the rapid geopolymerization. ETPS was well dried at 100±5 °C and ground to get particle size ranges between 90 μm and 2 mm prior to its application as a filler material. GBFS was milled in a ball mill for two hours to get the desired particle size ($d_{50} = 8.83 \mu\text{m}$) before use. Analytical grade sodium hydroxide pellet (NaOH) with 97% purity was provided by M/S NICE Chemicals, India. Commercial grade sodium silicate solution (Na_2SiO_3) with composition Na₂O 14.7%, SiO₂ 29.4% and H₂O 55.9% was used.

Mix proportions and methods

The alkaline activator was a mixture of NaOH solution and Na–silicate solution by volume and was prepared at least 24 hours prior to its use. The NaOH concentration and Na–silicate to NaOH (S/H) ratio were fixed to 6 M and 0.33 respectively. Table 1 shows the batch compositions of two blended geopolymers: FA+GBFS+ETPS (Batch 1) and FA+AOD+ETPS (Batch 2). The Liquid to solid ratio of 0.50 was

used in making all the geopolymer samples. The chemical analysis of raw materials was done using Inductive coupled plasma optical emission spectroscopy (VARINA, VISTA-MPX CCD simultaneous ICP – OES). The fineness of raw materials was ascertained using

sieve analysis method. The mineralogical phases were studied using the XRD patterns obtained by Powder X-ray Diffraction technique using $\text{CuK}\alpha$ radiation with Fe filter (X-ray BRUKER Diffractometer, Model: D8 Discover).

Table 1 Geopolymer batch compositions

Batch 1				Batch 2			
Sample code	FA %	ETPS %	GBFS %	Sample code	FA %	ETPS %	AOD %
G1F4E5	40	50	10	A1F4E5	40	50	10
G1F3E6	30	60	10	A1F3E6	30	60	10
G1F2E7	20	70	10	A1F2E7	20	70	10
G1F1E8	10	80	10	A1F1E8	10	80	10
G1F0E9	0	90	10	A1F0E9	0	90	10
G2F3E5	30	50	20	A2F3E5	30	50	20
G2F2E6	20	60	20	A2F2E6	20	60	20
G2F1E7	10	70	20	A2F1E7	10	70	20
G2F0E8	0	80	20	A2F0E8	0	80	20

For the compressive strength of geopolymer, the dry materials (FA+GBFS+ETPS) or (FA+AOD+ETPS) were blended or mixed properly in a mechanical mixer for 3 minutes and then the alkaline activator was added and mixed for further 3 minutes. The samples were vibro-casted in 43 mm diameter cylindrical mould. The samples with mould were kept at 50°C for 24 h, just after the casting. The samples were demoulded after heat curing and kept in a sealed condition at ambient temperature for 28 d. The compressive strength of the samples after 28 d was determined using Automatic Compression Testing Machine (AIMIL COMPTEST 2000, India). The durability of geopolymer samples was tested by immersing specimens in 0.1 Molar (M) acid solutions (H_2SO_4 , HCl, and HNO_3) over a period of 28 d and finally testing the compressive strength of specimens. To keep a constant pH, acid solutions were replaced after 14 days. The samples used in durability test were prepared similarly to compressive strength test. The samples were cured at 50°C for 24 h and then kept in ambient conditions for 28 d. After the completion of 28 d, the samples were immersed in acid solutions for further 28 d. After 28 days, the specimens were dried and then tested for compressive strength to find the % loss of strength before and after the acid attack. The geopolymerization reaction was recorded on isothermal conduction calorimeter (TAM AIR, Thermometric AB, Jarafalla, Sweden) at 27°C for a period of 24 h. The mineralogical characterization of geopolymer samples after 28 d was done using Powder X-ray Diffraction technique using $\text{CuK}\alpha$ radiation with Fe filter (X-ray BRUKER diffractometer, model: D8 Discover). The morphological characterization of the fractured surface of geopolymer samples after 28 d was done by a NOVA Scanning Electron Microscope (FEI-430, NOVA) with an EDAX attachment for X-Ray microanalysis.

Results and discussion

Material characterization

Chemical compositions of fly ash, GBFS and AOD slag are provided in Table 2. The major oxides in the case of fly ash are SiO_2 , Al_2O_3 and Fe_2O_3 , which is around 90.37% in total. The calcium oxide content in fly ash is less than 10%. Hence, it can be classified as Class–F fly ash as per ASTM C618–2000¹³ or BIS: 3812(Part–I)–2003.¹⁴ The fly ash is

mainly alumino–silicate in nature with $\text{aSiO}_2/\text{Al}_2\text{O}_3$ ratio around 1.72. The major oxides in GBFS are CaO and SiO_2 , which are the result of the addition of limestone and for sterite or dolomite as a flux in their production process. GBFS is frequently used as blending materials with Portland cement to make Portland Slag cement.¹⁵ GBFS is also known for improving the rate of geopolymerization and strength development in making geopolymer.^{7,8} The CaO content in AOD slag is high, which is a result of lime addition during AOD process. The SiO_2 is second dominating oxide followed by K_2O , Al_2O_3 and MgO , which comes from the flux addition and refractory lining.⁹ The Oxide of Chromium is also observed but in very low concentration.

Table 2 Chemical compositions of fly ash, GBFS and AOD slag

Component (%)	Fly ash	GBFS	AOD
SiO_2	51.06	32.97	33.39
Al_2O_3	29.71	17.97	3.52
Fe_2O_3	9.6	0.72	0.48
CaO	2.14	35.08	47.78
MgO	0.75	10.31	2.4
Na_2O	0.56	--	--
K_2O	0.4	--	11.02
Cr_2O_3	--	--	0.92
LOI	0.6	0.58	--

Table 3 presents the chemical composition of ETPS. ETPS is highly rich in iron content. The higher amount of iron oxide makes it red in color. The chemical components of ETPS are very different from other materials used in this study. The oxides of Ca, Al, and Si are absent and it shows the low reactivity or inert nature of ETPS. The specific gravity of fly ash, AOD slag, GBFS and ETPS was 1.97, 3.03, 2.88 and 2.46 respectively. Figure 1 presents the fineness curve of fly ash, AOD slag, and GBFS. The results suggest that the AOD slag contains coarser particles than fly ash and GBFS. The GBFS contains

a high amount of finer particles among others. Figure 2 shows the XRD patterns of fly ash, GBFS, AOD slag and ETPS. The major peaks identified in fly ash and AOD slag are Quartz and Mullite. The crystalline phase formed in GBFS is gelignite ($\text{Ca}_2\text{Al}(\text{AlSiO}_7)$) only. The main mineralogical phase in ETPS is Srebrodolskite ($\text{Ca}_2\text{Fe}^{3+}_2\text{O}_5$) and no other phases are seen.

Table 3 Chemical compositions of ETPS

Component (%)	ETPS
MnO_2	0.727
CdO	0.005
Fe_2O_3	85
ZnO	10.057
PbO	4.041
Cr_2O_3	0.056
CuO	0.012

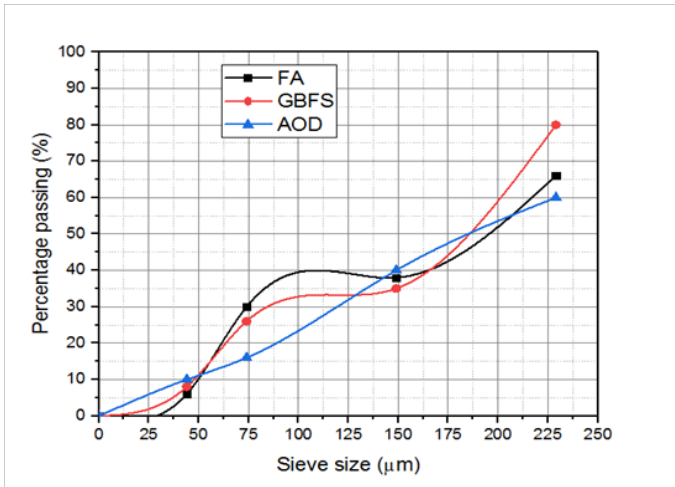


Figure 1 Fineness curve of FA, GBFS and AOD.

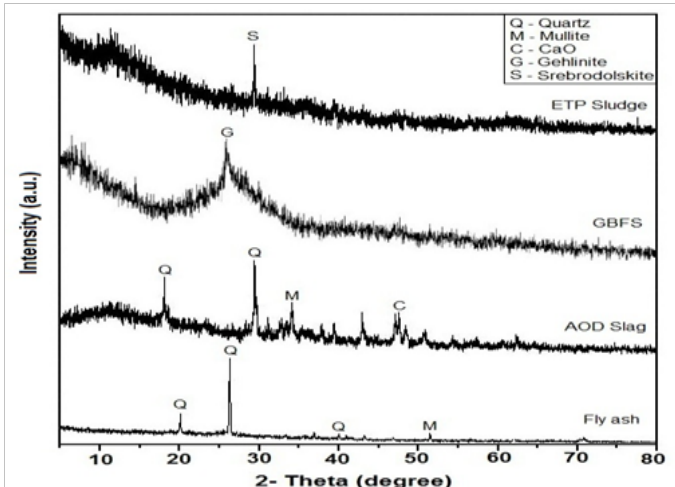


Figure 2 XRD patterns of fly ash, AOD Slag, GBFS, and ETPS.

Geopolymer characterization

Compressive strength

Figure 3 shows the compressive strength of geopolymer samples with 10% AOD slag and 10% GBFS. The compressive strength decreases with the increasing percentage of ETPS in all the samples. This decrease in strength is due to the inert or low reactivity of ETPS, which is acting as filler material. The compressive strength of geopolymer samples with 20% AOD slag and 20% GBFS is presented in Figure 4. The similar results are seen in both AOD slag and GBFS based samples. The only difference is the lower compressive strength of AOD slag based sample with respect to that of GBFS based sample. This may be attributed to the high reactivity and fineness of GBFS in comparison with AOD slag.⁸ Also, GBFS may lead to the formation of additional reaction products such as C–S–H and improve the strength.⁸ Although the formation of C–S–H may also be there in AOD slag based samples but not upto that extent such in the case of GBFS.⁹ It is evident by the XRD of AOD slag (crystalline nature), where apart from quartz and mullite, the peak of calcite (CaO) phases was also observed. The maximum strength developed was around 17.5 MPa in sample G2F3E5. This is mainly due to the high percentage of GBFS (20%) and fly ash (30%), which leads to the formation of reaction products. The minimum strength developed was around 3.8 MPa in sample A1F0E9. The compressive strength of fly ash–slag–sludge geopolymer is in the range of 3.8–17.5 MPa, which limits its application. It can be used in manufacturing structural units such as bricks, hollow and solid concrete blocks, hollow and solid lightweight concrete blocks, etc. These units require compressive strength in the range 3.5–15 MPa as per BIS: 1077–1992, BIS: 2185 (1)–1993, BIS: 2185 (2)–1993.

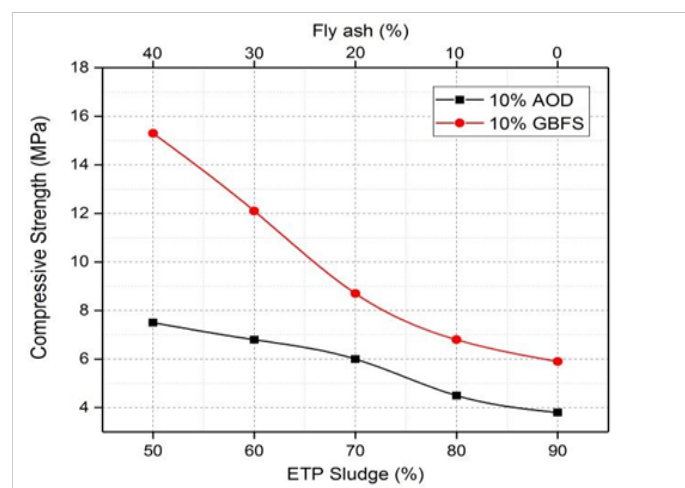


Figure 3 Compressive strength of geopolymer samples with 10% AOD slag and 10% GBFS.

Durability test results

Table 4 shows the compressive strength and % loss of strength of geopolymer samples after immersion in acid solutions. In the case of 10% and 20% AOD slag samples, the complete loss of strength is seen. This result shows that the AOD slag based samples have poor resistance toward acid attack. In the case of 10% and 20% GBFS samples, the maximum effect of the acid attack is caused by 0.1M H_2SO_4 solution and the minimum effect by the 0.1M HNO_3 .

solution. This is because of the low pH of acid (0.1M H_2SO_4), which is responsible for the highest chemical attack.¹⁶ Allahverdi et al.,¹⁷ reported that the geopolymers are less vulnerable to nitric acid attack. Here, the minimum effect of the HNO_3 solution is in agreement with the result reported by them. The complete loss of strength is also observed in G1F1E8, G1F0E9, and G2F0E8 samples. The minimum % losses of strength are exhibited by G2F3E5 samples, which are 9.2 %, 13.2 %, and 16.0 % by 0.1M HNO_3 , 0.1M HCl, and 0.1M H_2SO_4 respectively. The reason behind the loss of strength may be the depletion of sodium and calcium ions through leaching process caused by acid attack and weakening of the polymeric bonds (Si–O–Al).^{17–19} This may increase the porosity of binder and ultimately lower the strength.^{16–20} The complete loss of strength in all AOD slag based samples may be due to the higher depletion of sodium & calcium and higher porosity with respect to GBFS based samples. Also, the % loss of strength is more in the samples containing high ETPS content. This is just because of the inert nature of ETPS. The acid resistance of GBFS based samples is appreciable relative to AOD slag based samples.

Table 4 Durability test results of geopolymers samples

Samples	0.1M H_2SO_4	0.1M HCl	0.1M HNO_3
	Compressive strength, MPa (Loss %)		
G1F4E5	10.8 (29.4)	11.6 (24.2)	12.4 (19.0)
G1F3E6	9.5 (21.5)	9.9 (18.2)	10.5 (13.2)
G1F2E7	4.5 (48.3)	4.7 (46.0)	5.4 (38.0)
G2F3E5	14.7 (16.0)	15.2 (13.2)	15.9 (9.2)
G2F2E6	9.7 (23.0)	10.2 (19.0)	10.8 (14.3)
G2F1E7	5.8 (31.8)	6.0 (29.4)	6.5 (23.5)

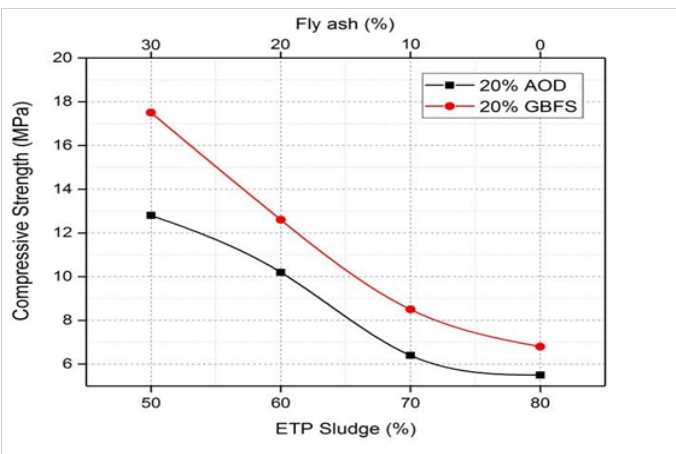


Figure 4 Compressive strength of geopolymers samples with 20% AOD slag and 20% GBFS.

Calorimetry studies

Figure 5 & Figure 6 presents the heat flow curves obtained by isothermal conduction calorimeter at 27°C for 24 h. The nature of curves is similar in all the samples. The complete reaction process consists of four stages – initial dissolution, induction, acceleration/deceleration and stable period.²¹ The heat evolution curves show two

calorimetric peaks: an initial peak (straight line) with significant high heat flow during the first few minutes and an acceleration peak with very low intensity at around 1 to 2 h. The first peak (initial straight line) corresponds to the wetting and partial dissolution of raw material and this is considered as physical phenomena.^{4,21,22} The second heat peak is very small and in few samples, it is not significant. The second peak is assigned to the formation of reaction products.^{21,23} GBFS based samples exhibit more intense peak than AOD slag based samples. This is due to high glass content and high reactivity of GBFS than AOD slag.⁸ This is evident by the XRD of GBFS and AOD slag. The higher content of ETPS decreases the main heat peak in all cases because of its very low reactivity or inert nature.

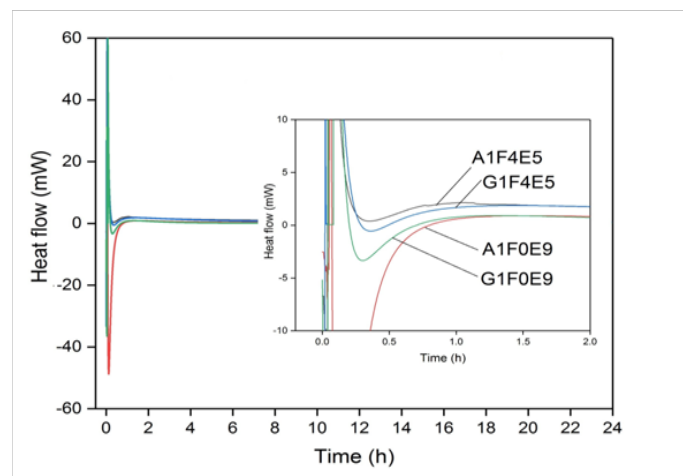


Figure 5 Heat evolution in geopolymers samples with 10% AOD slag and 10% GBFS.

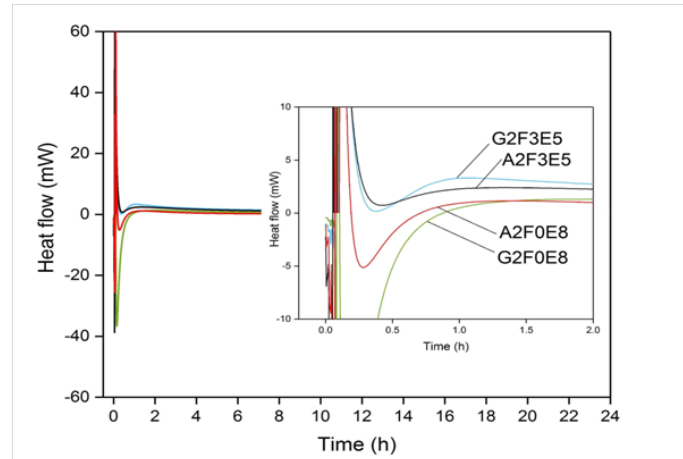


Figure 6 Heat evolution in geopolymers samples with 20% AOD slag and 20% GBFS.

Mineralogical characteristics

Figure 7 shows the XRD patterns of geopolymers samples with 10% AOD and 10% GBFS. The major peaks of Quartz and Mullite are observed, which are remnant from parent fly ash and AOD slag.²² The reaction products (A–S–H and C–S–H) formed by the geopolymers are amorphous or semi-crystalline in nature. The hump between 10° and 30° indicates the presence of amorphous or

semi-crystalline reaction products.⁷ No any crystalline phases other than Quartz and Mullite are observed. The absence of crystalline phases is observed in the samples having high ETPS content (least fly ash content), such in the case of G1F0E9. The similar results are observed in 20% AOD and 20% GBFS based geopolymer samples.

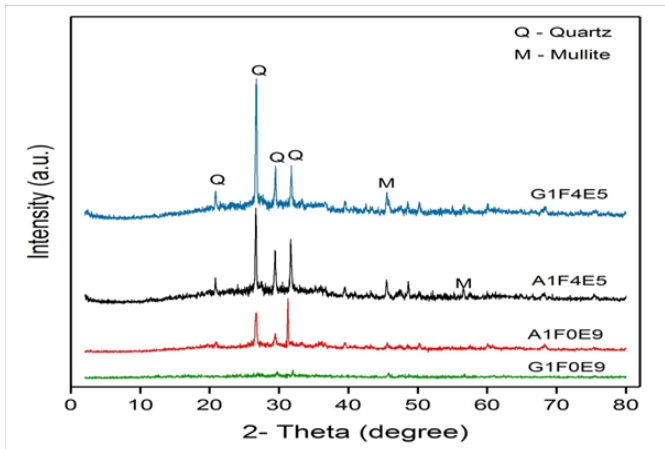


Figure 7 XRD patterns of geopolymer samples with 10% AOD slag and 10% GBFS.

Morphological characteristics

Figure 8a–d shows the morphology of selected geopolymer samples. The micro structural features observed are fully reacted matrix, dense gel phases and fibrous mass of C–S–H gel. The reaction products formed in both samples are A–S–H and C–S–H gel (A = Al_2O_3 , C = CaO, S = SiO_2 , H = H_2O). The main geopolymeric gel formed in case of fly ash based geopolymer is N–A–S–H gel.²⁴ But in present case, the presence of calcium, from slag in blended geopolymer, may lead to the formation of C–A–S–H gel and destroys the N–A–S–H gel structure to some extent by partially replacing Na with Ca to form (N,C)–A–S–H gel.^{21,25–27} For G1F4E5 and A1F4E5 samples, the main reaction products have the atomic ratios near to Si/Al = 2.29–3.03, Ca/Si = 0.14–0.34 and Al/Si = 1.01–3.10. This may indicate the formation of both C–A–S–H and N–A–S–H gel phases or one hybrid (N,C)–A–S–H gel phase. Both GBFS and AOD based samples exhibit almost similar morphological features. However, there may be the variation in the extent of reaction products. Because GBFS is highly amorphous than AOD slag and hence the formation of Ca-based reaction products is more in GBFS based geopolymer samples. Figure 8a shows the formation of gelatinous mass of N–A–S–H with the chemical composition of Si/Al = 2.96, Ca/Si = 0.17 and Al/Si = 1.98. The well reacted matrix of geopolymeric (A–S–H) gel is shown in Figure 8b. The fibrous mass of C–S–H gel having anatomic ratio close to Ca/Si = 0.95 is observed as shown in Figure 8c. The formation of C–A–S–H gel with chemical composition of Si/Al = 2.29, Ca/Si = 0.32 and Al/Si = 1.37 is also seen (Figure 8d). The presence of iron content is also observed in both samples, which is around 4.27 Atomic % in A1F4E5 and 3.08 Atomic % in G1F4E5. The iron content might get into the polymeric system to form ferro-sialate based reaction products.⁴ Kumar et al.,⁴ reported the existence of ferro-sialate based reaction product with Fe/Si ratio in the range of 0.20–5.02. But in the present case, the Fe/Si ratio is in the range of 0.15–0.29 which comes in lower range. This confirms that the iron from ETPS does not alter the structure of reaction products due to its very low reactivity.

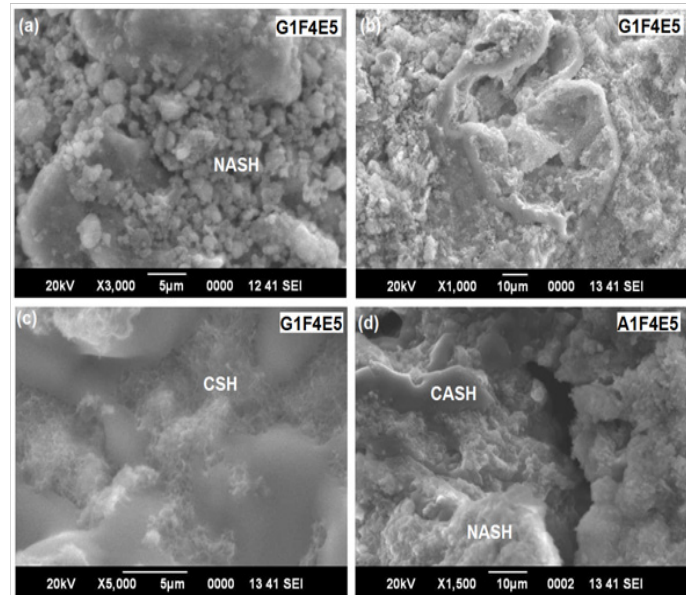


Figure 8 SEM images of GBFS and AOD based geopolymer samples.

Conclusion

This paper investigates the potential of ETP sludge as a filler material in fly ash–slag based geopolymer and the role of AOD slag and GBFS in fly ash–slag–sludge blended geopolymer. The fly ash–slag–sludge blend was activated with 6 M NaOH & Na–silicate at 50°C curing temperature for 24 h period.²⁴

The following conclusions can be drawn based on the present study:

1. The ETP sludge has very low reactivity and it does not participate in the geopolymerization process. But it can be used as filler material in fly ash–slag blended geopolymer. The compressive strength of different compositions was observed in the range of 3.8 to 17.5 MPa. The fly ash–slag–sludge blended geopolymer can be used in making building brick and hollow & solid concrete block. The durability results show that the AOD slag based samples have poor resistance towards acid attack whereas the appreciable result of the acid attack is exhibited by GBFS based samples.
2. The nature of calorimetric curves obtained is similar in all samples. The intense peaks appear with an increase in slag content. GBFS based samples show an intense peak at a lower time with respect to AOD slag based samples. The higher content of ETP sludge decreases the main heat peak.
3. The major reaction products observed in GBFS and AOD based samples are C–A–S–H, N–A–S–H, (N,C)–A–S–H gel and C–S–H gel. EDAX analysis also shows the presence of Fe in both samples, which is remnant from parent ETPS.

Acknowledgements

The authors want to cordially acknowledge the Director, National Institute of Foundry and Forge Technology, Ranchi, Director, BIT Sindri and Director IIT (ISM) Dhanbad for their kind permission to publish this paper. The fly ash, GBFS, AOD slag, and ETP sludge

were received from Tata Power Limited, Jojobera Plant, Jharkhand (India); Tata Steel, Jamshedpur (India); Jindal Steel & Power Limited, Jajpur, Odisha (India); and Usha Martin Ranchi Unit, Jharkhand (India) respectively; this is gratefully acknowledged.

Conflict of interest

No potential conflict of interest was reported by the authors.

References

1. Davidovits J. *Geopolymer Cement, a review*. Geopolymer Inst. Libr. 2013:1–11.
2. Provis JL, Van Deventer JSJ. *Introduction to geopolymers*. Woodhead Publishing Limited, USA; 2002.
3. Provis JL. Geopolymers and other alkali activated materials : why ,how , and what ?, *Mater Struct*. 2014;47(1-2):11–25.
4. Kumar S, Yankwa Djobo JN, Kumar A, et al. Geopolymerization behavior of fine iron-rich fraction of brown fly ash. *J Build Eng*. 2016;8:172–178.
5. Djobo JNY, Elimbi A, Tchakoute HK, et al. Mechanical activation of volcanic ash for geopolymer synthesis: effect on reaction kinetics, gel characteristics, physical and mechanical properties. *R Soc Chem*. 2016;6:39106–39117.
6. Nath SK, Kumar S. Influence of iron making slags on strength and microstructure of fly ash geopolymer. *Constr Build Mater*. 2013;38:924–930.
7. Sinha DK, Kumar A, Kumar S. Development of Geopolymer Concrete from Fly Ash and Bottom Ash Mixture. *Trans Indian Ceram Soc*. 2014;73(2):143–148.
8. Kumar S, Kumar R, Influence of granulated blast furnace slag on the reaction, structure and properties of fly ash based geopolymer. *J Mater Sci*. 2010;45(3):607–615.
9. Salman M, Cizer Ö, Pontikes Y, et al. Alkali Activation of AOD Stainless Steel Slag Under Steam Curing Conditions. *J Am Ceram Soc*. 2015;98(1):3062–3074.
10. Balasubramanian J, Sabumon PC, Lazar JU, et al. Reuse of textile effluent treatment plant sludge in building materials. *Waste Manag*. 2006;26(1):22–28.
11. Saikia NJ, Sengupta P, Gogoi PK, et al. Cementitious properties of metakaolin-normal Portland cement mixture in the presence of petroleum effluent treatment plant sludge. *Cem Concr Res*. 2002;32(11):1717–1724.
12. Firdous S, Naveen Saharan E. A Review Study on Application and Strength of Concrete with ETP Sludge and lathe waste. *Int J Latest Res Eng Comput*. 2017;5(3):25–28.
13. ASTM C618-12a. *Standard Specification for Coal Fly Ash and Raw or Calcined Natural Pozzolan for Use in Concrete*. ASTM Int. West Conshohocken, PA, 2012.
14. BIS:3812-1981. *Specification for fly ash for use as pozzolana and admixture*. Bur Indian Stand. New Delhi, India; 1992.
15. BIS:455-2005. *Portland Slag Cement – Specification*. Bur Indian Stand. New Delhi, India; 2005.
16. Shi C, Stegemann J. Acid corrosion resistance of different cementing materials. *Cem Concr Res*. 2000;30(5):803–808.
17. Allahverdi F Škvára. *Nitric Acid Attack on hardened Paste of Geopolymeric Cements (Part 1)*. Ceram Silikaty. 2001;45:81–88.
18. Allahverdi F Škvára. *Nitric acid attack on hardened paste of geopolymeric cements (Part 2)*. Ceram Silikaty. 2001;45:143–149.
19. Allahverdi F Škvára. *Sulfuric Acid Attack on Hardened Paste of Geopolymer Cements Part 1. Mechanism of Corrosion at Relatively High Concentrations*. Ceram Silikaty. 2005;45:225–229.
20. Pacheco-torgal F, Abdollahnejad Z, Camões AF, et al. Durability of alkali-activated binders : A clear advantage over Portland cement or an unproven issue ?, *Constr Build Mater*. 2012;30:400–405.
21. Gao X, Yu QL, Brouwers HJH. Reaction kinetics, gel character and strength of ambient temperature cured alkali activated slag-fly ash blends. *Constr Build Mater*. 2015;80:105–115.
22. Kumar S, Kumar R. Mechanical activation of fly ash : Effect on reaction, structure and properties of resulting geopolymer. *Ceram Int*. 2011;37(2):533–541.
23. Nath SK, Maitra S, Mukherjee S, et al. Microstructural and morphological evolution of fly ash based geopolymers. *Constr Build Mater*. 2016;111:758–765.
24. García-Lodeiro A, Fernández-Jiménez A, Palomo DE, et al. Effect of calcium additions on N-A-S-H cementitious gels. *J Am Ceram Soc*. 2010;39:1934–1940.
25. Ismail SA, Bernal JL, Provis R, et al. Modification of phase evolution in alkali-activated blast furnace slag by the incorporation of fly ash. *Cem Concr Compos*. 2014;45:125–135.
26. Criado M, Aperador W, Sobrados I. Microstructural and mechanical properties of alkali activated Colombian raw materials. *Materials*. 2016;9(3):158.
27. Davidovits F, Davidovits J, Davidovits M. Geopolymer cement of the calcium ferro-aluminosilicate polymer type and production. India; 2013.